

# Wearable Organic Electrochemical Transistor Array for Skin-Surface Electrocardiogram Mapping Above a Human Heart

Anneng Yang, Jiajun Song, Hong Liu, Zeyu Zhao, Li Li, and Feng Yan\*

Electrocardiogram (ECG) mapping can provide vital information in sports training and cardiac disease diagnosis. However, most electronic devices for monitoring ECG signals need to use multiple long wires, which limit their wearability and conformability in practical applications, while wearable ECG mapping based on integrated sensor arrays has been rarely reported. Herein, ultra-flexible organic electrochemical transistor (OECT) arrays used for wearable ECG mapping on the skin surface above a human heart are presented. QRS complexes of ECG signals at different recording distances and directions relative to the heart are obtained. Furthermore, the ECG signals are successfully analyzed by the devices before and after exercise, indicating potential applications in some sports training and fitness scenarios. The OECT arrays that can conveniently monitor spacial ECG signals in the heart region may find niche applications in wearable electronics and healthcare products in the future.

\$2 billion by the end of 2030 as predicted.<sup>[8]</sup> Currently, clinical ECG signals are acquired through a 12-lead ECG recorder that requires multiple-wire connection to different sites of the human body. The 12-lead ECG is usually used for centralized measurement under the operation of experienced specialists due to its high accuracy and safety while it is unwieldy, expensive, and complicated for personal use.<sup>[9]</sup> Some portable ECG recorders have been developed and utilized in recent years, in which three wires of the recorder are connected to three different sites of human body to realize 1-lead ECG monitoring during personal and sports training. Although 1-lead ECG recorders are much more portable than 12-lead ones, the multiple wires (at

## 1. Introduction

Wearable bioelectronics enables various electrophysiological signal recordings, benefitting personal health monitoring.<sup>[1–3]</sup> Among these electrophysiological signals, electrocardiogram (ECG) can provide valuable information in cardiac monitoring and the diagnosis of heart-related diseases, such as arrhythmias, ischemia, and elderly heart failure.<sup>[4–7]</sup> Moreover, the market size of cardiac monitoring by flexible electronics will reach

at least three wires) connecting to the electrode patches on three limbs could be inconvenient and uncomfortable for human to wear them.<sup>[10]</sup> The wearable ECG patches with less wires and miniaturized structure are urgently needed in many practical applications. For example, wearable ECG sensors in the form of one integrated device can provide portable and comfortable ECG monitoring in sports training and predictive diagnostics, which shows huge potential in telehealth management.<sup>[11]</sup> At the same time, the heart malfunction can be warned in advance and treatment can be timely applied by implanted/external pacemakers to extend precious rescue time during ECG monitoring.<sup>[12]</sup>


Conventionally, electrophysiological signals are acquired through potentiometric technique by using low-impedance electrodes, which are further processed by external equipment to obtain high-quality signals.<sup>[11,13,14]</sup> Ag/AgCl electrode is one of the most widely used electrodes in ECG recording scenarios because of its low impedance and non-polarization properties.<sup>[5,9,15]</sup> Recently, novel ECG patches have been developed to decrease contact impedance and increase its conformability on the skin, thus realizing long-term, sensitive and reliable ECG recording. The electrode patches with different functions, such as, conformal textile structure, water resistance, and anti-dermal-surface lipid, have been widely used for ECG signal monitoring.<sup>[10,16,17]</sup> Roger's group fabricated wireless skin-interfaced sensors, which integrated the ECG sensor with other sensors for vital sign monitoring in intensive-care units, especially in neonatal and pediatric care.<sup>[11,18]</sup> Wearable ECG mapping through an array can provide useful information as it can capture multichannel signals in a short period.<sup>[19]</sup> Currently, in order to obtain high-quality signals, most ECG mapping arrays directly adhere on the surface of a heart, which is invasive to test subjects and not suitable for wearable applications.<sup>[7,20]</sup> On

A. Yang, J. Song, H. Liu, Z. Zhao, F. Yan  
Department of Applied Physics  
The Hong Kong Polytechnic University  
Hung Hom, Kowloon, Hong Kong SAR 999077, P. R. China  
E-mail: apafyan@polyu.edu.hk

A. Yang  
Faculty of Science  
Kunming University of Science and Technology  
Kunming, Yunnan 650032, P. R. China

L. Li  
School of Fashion and Textiles  
The Hong Kong Polytechnic University  
Hung Hom, Kowloon, Hong Kong 999077, P. R. China

F. Yan  
Research Institute of Intelligent Wearable Systems  
The Hong Kong Polytechnic University  
Hung Hom, Kowloon, Hong Kong SAR 999077, P. R. China

 The ORCID identification number(s) for the author(s) of this article can be found under <https://doi.org/10.1002/adfm.202215037>.

© 2023 The Author(s). Advanced Functional Materials published by Wiley-VCH GmbH. This is an open access article under the terms of the Creative Commons Attribution License, which permits use, distribution and reproduction in any medium, provided the original work is properly cited.

DOI: 10.1002/adfm.202215037

the other hand, the introduction of a multi-wire layout in the novel ECG patches inevitably increases device complexity.<sup>[11,21]</sup>

Recently, organic electrochemical transistors (OECTs) are emerging as excellent tissue-electronics interfaces due to their outstanding ion-to-electron transducing efficiency and good biocompatibility.<sup>[22,23]</sup> Poly(3,4-ethylenedioxythiophene) : polystyrene sulfonate (PEDOT:PSS) is commonly used in OECTs due to its excellent carrier mobility and volumetric charge storage capacity.<sup>[24–26]</sup> Benefitting from the volumetric capacitance of hydrophilic PEDOT:PSS channel, the OECTs show ultrahigh transconductance. The intrinsic signal amplification capability of the OECTs make them possible for weak electrophysiological signal monitoring.<sup>[27–31]</sup> Campana et al first applied the device into ECG monitoring although high noise existed in the recorded signal.<sup>[14]</sup> After that, different OECT devices were further developed and used for ECG recordings.<sup>[6,7,32–36]</sup> However, the miniaturized and wearable ECG sensor array based on OECT is rarely reported. Here, we present a flexible OECT array with response time less than 30  $\mu\text{s}$ , which can conform on the skin of a human subject above the heart to perform wearable ECG signal mapping. Due to the high amplification capability of OECTs, the spatial variation of ECG signals on the skin surface above the heart can be accurately measured. The flexible and integrated OECT array shows huge potential in wearable and portable ECG monitoring in the future.

## 2. Results and Discussion

As shown in **Figure 1a,b**, a flexible OECT consists of a parylene supporting layer, gold interconnection, a SU-8 photoresist layer

for encapsulation, and a PEDOT:PSS organic channel layer. In order to achieve its conformability on an arbitrary surface, the device was fabricated on the ultra-thin parylene substrate (thickness:  $<2 \mu\text{m}$ ). An ion gel is coated on the channel and gate area of the device to form good contacts between the device and a human skin. The SU-8 layer is optimized to reach a similar thickness to the parylene layer ( $\approx 2 \mu\text{m}$ ), so the gold interconnection is sandwiched at the neutral-plane position to achieve a high bending stability (**Figure 1c**). One layer of PEDOT:PSS is drop-coated on the gate electrode of the device to decrease interface impedance between the electrolyte and gate electrode. The gate area is much larger than the channel area (more than 1000 times) so that effective gating of the device can be achieved.<sup>[24,27]</sup> **Figure 1d** shows the transfer characteristics ( $I_D$  vs  $V_G$ ) of an ultra-flexible OECT, which was bent for more than 500 times with a bending radius of 0.5 mm. Notably, the performance degradation of the device is very little. Moreover, the device shows good conformability when bending along a thin wire (**Inset of Figure 1d**). The excellent bending stability and conformability of the devices are key to achieving reliable ECG monitoring on human skin.

**Figure 2a,b** shows the transfer ( $I_D$  vs  $V_G$ ) and output characteristics ( $I_D$  vs  $V_D$ ) of a flexible OECT. The drain voltage  $V_D$  is 0.05 V for transfer characterization unless otherwise specified. The device shows a ON/OFF ratio of more than 100 and a maximum transconductance of 0.26 mS at  $V_G = 0.48 \text{ V}$  and  $V_D = 0.05 \text{ V}$ . The device transfer performance tested in ion gel is similar to that in an electrolyte (**Figure S1a**, Supporting Information) due to their similarity in ionic composition and concentration. The gate leakage current is more than three orders of magnitude lower than the channel current (**Figure S1b**, Supporting Information).

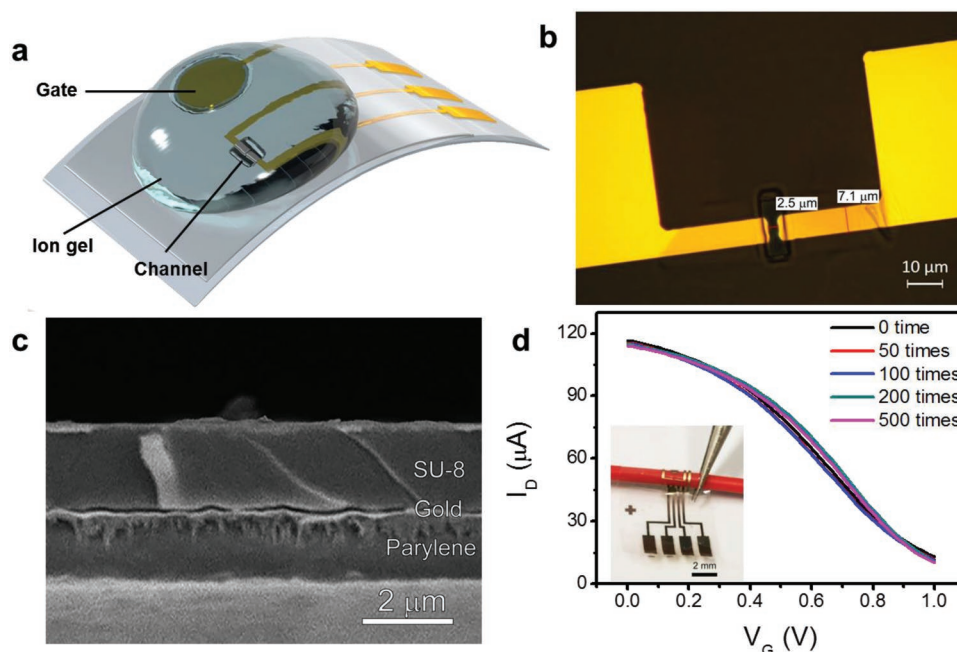


**Figure 1.** a) Illustration of a short-channel OECT with a channel length and width of  $\approx 2$  and  $8 \mu\text{m}$ , respectively. b) Micrograph of the channel part of an OECT. c) Sandwich structure of ultra-flexible OECT that consists of SU-8 package layer, gold layer, and parylene substrate layer, respectively. d) Transfer characteristics ( $I_D$  vs  $V_G$ ) of an ultra-flexible OECT after bending for different times with a bending radius of 0.5 mm.  $V_D = 0.05 \text{ V}$ . Inset: bending status of the device along a wire.

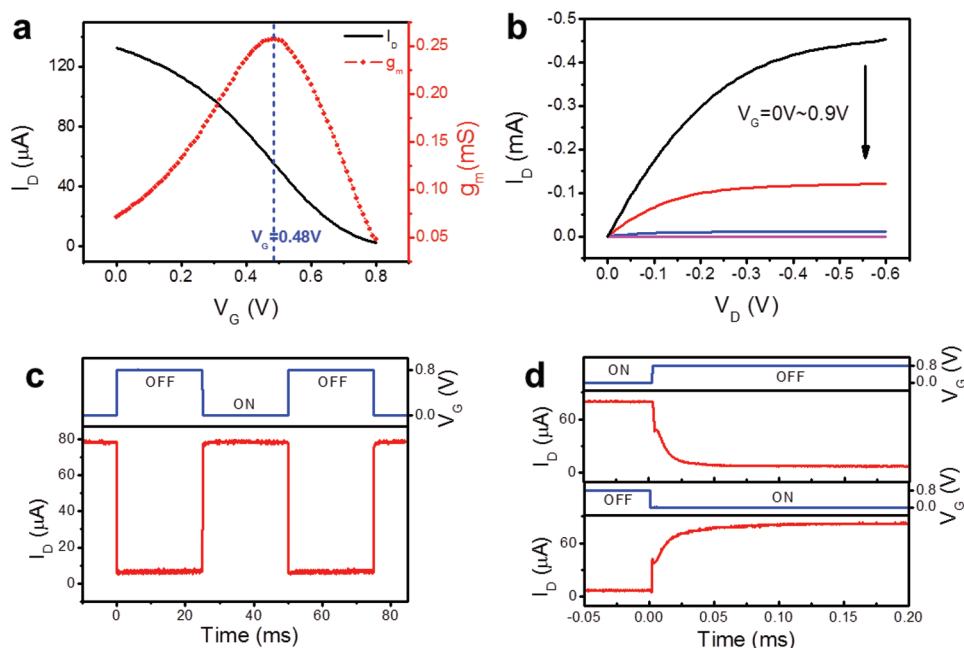


**Figure 2.** a) Transfer and b) output curves of a short channel OECT characterized in ion gel. For transfer test,  $V_D = 0.05$  V, scanning rate is  $20$  mV  $s^{-1}$ . c,d) Transient channel current response of a short-channel OECT gated by pulses which shows on-to-off and off-to-on switches.  $V_D = 0.05$  V.

Response speed of an OECT is a key factor in ECG monitoring because a time resolution within several milliseconds is needed. In order to confirm whether the response speed of the device can meet the requirements of ECG signal recording (minimum sampling frequency should be more than  $120$  Hz<sup>[37]</sup>), the transient properties of our OECTs are characterized. As shown in Figure S3 (Supporting Information), the channel length of an OECT can influence its response speed. We can find that the response time decreases from  $0.53$  to  $0.1$  ms when the channel length is changed from  $30$  to  $10$   $\mu\text{m}$ . In order to further decrease its response time, the channel length of the device is further decreased to  $\approx 2$   $\mu\text{m}$ , as shown in Figure 1b, which is much shorter than those reported previously.<sup>[38,39]</sup> As shown in Figure 2c, the transient response of the channel current is characterized in ion gel and its long-term stability was confirmed by applying pulses for more than one hour. According to the exponential fit curve in Figure 2d, the device response time of on-to-off ( $\tau_{\text{OFF}}$ ) and off-to-on ( $\tau_{\text{ON}}$ ) are  $\approx 36$  and  $51$   $\mu\text{s}$ , respectively. Notably,  $\tau_{\text{OFF}}$  and  $\tau_{\text{ON}}$  are different due to the different de-doping and doping process in the channel, which is consistent with previous reports about the asymmetric ion diffusion behavior of a typical OECT device.<sup>[40,41]</sup> Moreover, as shown in Figure S4 (Supporting Information), the response time can be further decreased from  $66$  to  $10$   $\mu\text{s}$  with the increase of electrolyte (NaCl) concentration from  $0.1$  to  $6$  mol  $L^{-1}$ , which confirms that the device response speed is ion-sensitive.<sup>[39,42]</sup> Hence, the response times of the  $2$ - $\mu\text{m}$  OECT are much shorter than those of previously reported OECTs used in electrophysiological signal monitoring.<sup>[14,27,39,43]</sup> For high-resolution ECG wave recording, the sampling frequency should be as high as  $1000$  Hz ( $t < 1$  ms), which can be achieved by our devices.<sup>[44]</sup>

The carrier transit time ( $\tau_t$ ) across the organic channel can be calculated according to the equation:  $\tau_t = L^2/\mu V_D$ , where  $L$

is channel length ( $L = 2$   $\mu\text{m}$ ),  $\mu$  is PEDOT:PSS hole mobility.<sup>[42]</sup> The hole mobility for PEDOT:PSS is usually in the range of  $1$ – $0.1$   $\text{cm}^2 \text{V}^{-1} \text{S}^{-1}$ .<sup>[45]</sup> So,  $\tau_t$  is in the range of  $0.8$ – $8$   $\mu\text{s}$ , which is much faster than the response time of the device shown in Figure 2d. Hence, the response speed of the OECT is limited by the ion transfer process across the electrolyte and the porous organic channel. In addition, we found that the response time is quite similar when the gate electrode and channel of an OECT were placed at different distances on a human subject (Figure S5, Supporting Information). According to the circuit model of a human body, the impedance of epidermis can be regarded as a resistor and a capacitor connected in parallel, which is much larger than the body impedance.<sup>[46]</sup> Therefore, it is reasonable to find that the distance between the gate electrode and the channel has little effect on their response speed and more attention should be paid to decrease interface impedance between the device and skin surface.<sup>[17]</sup>

The ECG signal stems from the muscular tissue of a heart, where pacemaker cells can spontaneously induce an influx of  $\text{Ca}^{2+}$  and further cause cell depolarization. This signal quickly spread to the whole heart area, thus causing rhythmic heart expansion and contraction, which is called the cardiac cycle. The macroscopic ion flux wave during the cardiac cycle leads to a tiny change of skin potential ranging from one to several of millivolts. The periodic potential changes spread from the heart area to limbs, which can be recorded as ECG signals. Abnormal waves in ECG monitoring, such as abnormal shapes and/or durations of QRS complex, T wave, and P wave, can be used for the diagnosis of some cardiac diseases.<sup>[46]</sup> For example, an unusually tall/low QRS complex may represent left ventricular hypertrophy or pericardial effusion infiltrative myocardial disease. A wide QRS duration (longer than  $120$  ms) may suggest the disruption of the heart conduction system. Normally, the

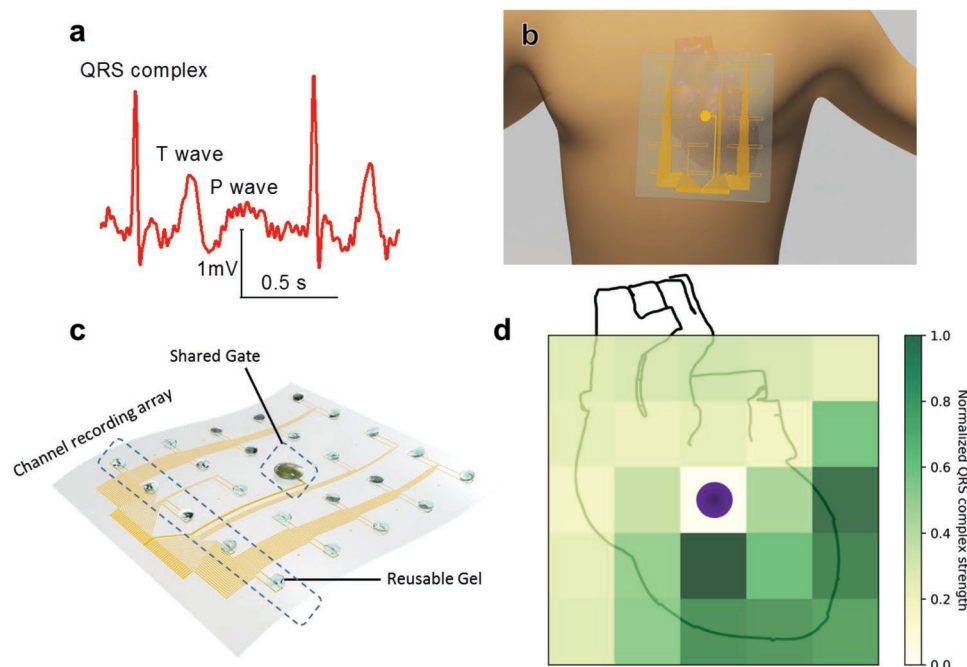


**Figure 3.** a) A representative ECG wave captured by a short channel OECT between the heart region and the forearm of a subject. b) Illustration of a flexible OECT array that can conformably adhere on a human body for ECG mapping. c) Illustration of flexible OECT array equipped with 24 channels and 1 shared gate electrode covered with reusable gel. The distance of adjacent channels/gate is 2.5 cm. d) Heat map of normalized ECG QRS complex signal strength captured by the OECT array.

duration of *P* wave is less than 80 ms. Typically, a large right atrium gives a tall and peaked *P* wave while a large left atrium gives a two-humped bifid *P* wave. Inverted or peaked *T* waves can be a sign of myocardial ischemia or hyperkalemia. All the ECG signals can be recorded by a potentiometer through low impedance electrodes.<sup>[47,48]</sup>

A typical ECG wave was recorded by an OECT device, as shown in **Figure 3a**, where gate and channel parts of the device are adhered above the heart and on the forearm, respectively. QRS complex peaks, *P* wave, and *T* wave are well duplicated, and its signal-to-noise ratio (SNR = 42.5 dB) can meet the requirements of functional ECG recording. The QRS complex contains the most obvious peaks in a typical ECG wave, which represents quick ventricular depolarization and is used to calculate heart rate. The rounded *P* and *T* waves represent atrial depolarization and ventricular repolarization, respectively. The duration of QRS complex is between 0.08–0.1 s, which confirms that the ventricular-paced rhythm of the human subject is normal.<sup>[46]</sup>

According to Einthoven's triangle theory, the limb-lead ECG forms the basis of the hexaxial reference system in coronal plane (**Figure S6**, Supporting Information).<sup>[49,50]</sup> The ECG signals are recorded along six directions (Leads I to III, aVR, aVL, aVF), which can be used to determine the heart's electrical axis in coronal plane. In order to confirm ECG mapping capability of the OECT array in coronal plane, 5 × 5 array of ultra-flexible OECTs was adhered on the chest area of the subject as shown in **Figure 3b**. The gate electrode pad was on the skin above the heart of the human subject and 5 × 5 channel arrays (except one center gate) were positioned near center of heart (**Figure 3c**; **Figure S7**, Supporting Information). The solid

gel prepared by gelatin in mixed solution of PBS and glycerin was applied on each recording site to avoid cross talk among 24 channels. Notably, the static and transient performances of the device with solid gel guarantee its long-term and reliable ECG monitoring (**Figure S8**, Supporting Information). Because the OECT array is fabricated on an ultra-thin parylene film ( $\approx 2 \mu\text{m}$  thick), it can conform on the skin with good contacts between them (**Figure S7a**, Supporting Information). The signals for the potential difference between the gate electrode and each channel in the array will be recorded and used for ECG mapping analysis.

The ECG signals from 24 channels are collected via a multiplexing wire hub that is connected to an external instrument (**Figure S7b**, Supporting Information). The ECG signals are shown in **Figure S9** (Supporting Information) and the QRS complex can be clearly observed from all recorded ECG signals. According to the heat map of the normalized QRS complex amplitude during ECG mapping, we can find that the strongest QRS complex peaks appeared in the fourth quadrant (left bottom region), which is consistent with the ECG waves recorded by the hexaxial reference system, in which Lead II records ECG wave with maximum QRS complex peak (**Figure 3d**). According to a standard ECG report, the QRS complex amplitude of ECG waves recorded by Lead aVL is much smaller than that recorded by other Leads in the hexaxial reference system. This result is similar to the ECG mapping result shown in **Figure S7** (Supporting Information), in which the QRS complex amplitude of ECG waves is smaller in the direction around  $-45^\circ$  than that in other directions. So, the ECG mapping result by the OECT array is consistent with that recorded through a hexaxial reference system. Moreover, the



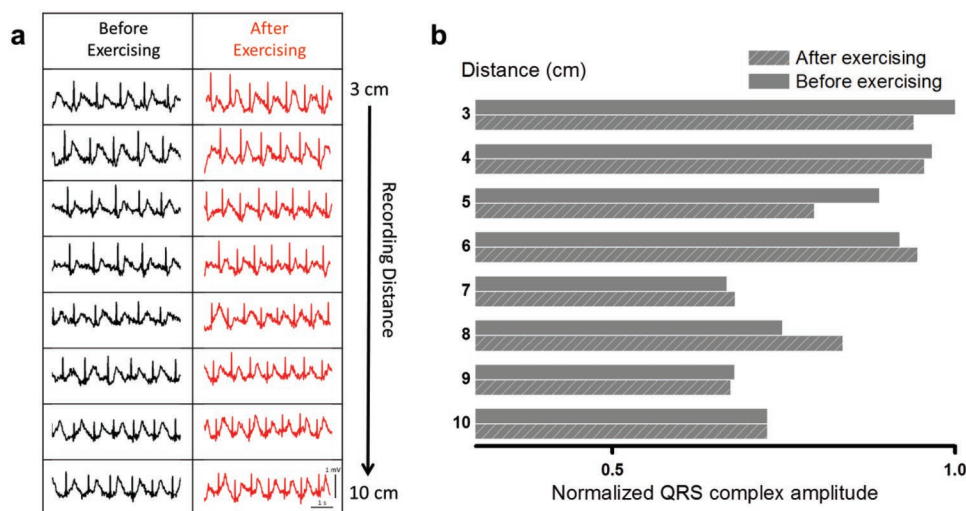


**Figure 4.** a) Representative ECG waves and b) normalized QRS complex amplitude distribution recorded along vertical direction of a heart with different recording distances between the gate and channel of OECT array before and after exercise. The gate is adhered on the center area above the heart in all measurements.

OECT array can perform ECG monitoring in a small area with high spatial resolution, which provides more accurate information for ECG signals.

Because maximum QRS complex peaks appear in the direction  $\approx 90^\circ$ , we further examined the ECG waves at different distances to the heart along this direction by an OECT array. A common gate electrode is placed on the skin above the heart center and multiple OECT channels are adhered on the recording sites (Figure S10a, Supporting Information). The ECG signal was first measured near the heart area within 10 cm range at 1 cm interval (RS3-RS10: 3 cm to 10 cm) and on the arm (RS30: 30 cm) and forearm (RS60: 60 cm), respectively. As shown in left column of Figure 4a; Figure S10b (Supporting Information), the representative ECG signals at different recording distances between the channel and gate (3 cm to 10 cm, 30 cm and 60 cm) of the device are presented. The QRS complex can be obviously observed in all recording sites. We can find that the QRS complex amplitude of ECG signal slowly increases with the decrease of recording distance from 10 to 3 cm. We hypothesize that the amplitude of the potential caused by the cardiac cycle spreads from the heart to limbs, so the recorded signal gets stronger with the decrease of the recording distance.

The sports effect on ECG monitoring was studied by medium exercising (stair climbing) of the human subject. Briefly, the ECG signals were recorded on RS3 to RS10 before and after stair climbing. As shown in Figure 4a, the ECG waves after exercising are quite similar to those before exercising while the heartbeat rate becomes faster after medium exercising (beats per minute (BPM) = 91, while resting BPM = 64). The QRS complex amplitude of the ECG waves behaves similarly in both situations, in which QRS complex amplitude reaches maximum at RS4 (Distance is 4 cm) after exercising while it reaches a maximum at RS3 (the distance is 3 cm) before exercising (Figure 4b). The duration of the QRS complex is a key indicator of the heart conduction system. As shown in Figure S11a (Supporting Information), the duration of QRS complex in all

recording sites before and after exercising are between 90 to 110 ms, which confirms the healthy heart conduction system of the tested subject. The duration of *P* waves in all recording sites before and after exercising are shown in Figure S11b (Supporting Information), which is between 230 and 390 ms. The duration of *P* waves become shorter after exercising in most recording sites (RS3-4, RS6-7, and RS10). No inverted *P* waves are observed, and a rounded peak appeared in all ECG waves. This confirms our device array is suitable for personal ECG mapping in sports training and exercise circumstances.

### 3. Conclusion

In summary, an ultra-flexible OECT array is successfully prepared by microfabrication technique and used for wearable ECG signal mapping. The channel length of a device can be shortened down to  $\approx 2 \mu\text{m}$ . The ON/OFF ratio of the device is more than 100, enabling its high detection sensitivity during ECG signal recording. The response time is as short as 10  $\mu\text{s}$ , which is sufficiently fast to record the fine structure of ECG waves and can provide accurate information for clinical diagnostics. The ECG signals mapped by the OECT array clearly show characteristic ECG peaks with the strength strongly dependent on recording sites. When the recording direction between the channel and gate is between  $0^\circ$  to  $90^\circ$ , the max QRS complex strength can be observed. The successful ECG mapping before and after exercising indicates its potential in some sports training and fitness scenarios. The OECT one-patch ECG mapping may provide a new concept for one integrated device in wearable and miniaturized ECG sensor design.

### Supporting Information

Supporting Information is available from the Wiley Online Library or from the author.

## Acknowledgements

This work is financially supported by the Research Institute of Intelligent Wearable Systems of the Hong Kong Polytechnic University, Hong Kong, China (Project Code: CD46) and the Research Institute for Sports Science and Technology of the Hong Kong Polytechnic University (Project Code: CD6X). The work was partially supported by the funding for Projects of Strategic Importance of the Hong Kong Polytechnic University (Project Code: 1-ZE2X). The work was partially supported by National Natural Science Foundation of China (Grant No. 62104088) and Yunnan Fundamental Research Projects, China (Grant No. 202201AU070144). The informed written consent from human participants or next of kin was obtained prior to the research.

## Conflict of Interest

The authors declare no conflict of interest.

## Data Availability Statement

The data that support the findings of this study are available from the corresponding author upon reasonable request.

## Keywords

ECG mapping, organic electrochemical transistors, wearable electronics

Received: December 26, 2022

Revised: January 17, 2023

Published online: February 2, 2023

- [1] J. Dunn, R. Runge, M. Snyder, *Pers. Med.* **2018**, *15*, 429.
- [2] T. T. Quang, L. Nae-Eung, *Adv. Mater.* **2016**, *28*, 4338.
- [3] T. Someya, Z. Bao, G. G. Malliaras, *Nature* **2016**, *540*, 379.
- [4] M. Ha, S. Lim, H. Ko, *J. Mater. Chem. B* **2018**, *6*, 4043.
- [5] S. Imani, A. J. Bhandokar, A. M. V. Mohan, R. Kumar, S. Yu, J. Wang, P. P. Mercier, *Nat. Commun.* **2016**, *7*, 11650.
- [6] S. Park, S. W. Heo, W. Lee, D. Inoue, Z. Jiang, K. Yu, H. Jinno, D. Hashizume, M. Sekino, T. Yokota, K. Fukuda, K. Tajima, T. Someya, *Nature* **2018**, *561*, 516.
- [7] W. Lee, S. Kobayashi, M. Nagase, Y. Jimbo, I. Saito, Y. Inoue, T. Yambe, M. Sekino, G. G. Malliaras, T. Yokota, M. Tanaka, T. Someya, *Sci. Adv.* **2018**, *4*, eaau2426.
- [8] Cardiac monitoring and CRM market size report, 2020–2027, **2020**. <https://www.grandviewresearch.com/industry-analysis/cardiac-monitoring-and-cardiac-rhythm-management-crm-market>, (accessed: July 2020).
- [9] Y. Yamamoto, D. Yamamoto, M. Takada, H. Naito, T. Arie, S. Akita, K. Takei, *Adv. Healthcare Mater.* **2017**, *6*, 1700495.
- [10] S. Ji, C. Wan, T. Wang, Q. Li, G. Chen, J. Wang, Z. Liu, H. Yang, X. Liu, X. Chen, *Adv. Mater.* **2020**, *32*, 2001496.
- [11] H. U. Chung, B. H. Kim, J. Y. Lee, J. Lee, Z. Xie, E. M. Ibler, K. Lee, A. Banks, J. Y. Jeong, J. Kim, C. Ogle, D. Grande, Y. Yu, H. Jang, P. Assem, D. Ryu, J. W. Kwak, M. Namkoong, J. B. Park, Y. Lee, D. H. Kim, A. Ryu, J. Jeong, K. You, B. Ji, Z. Liu, Q. Huo, X. Feng, Y. Deng, Y. Xu, et al, *Science* **2019**, *363*, eaau0780.
- [12] E. B. Fortescue, C. I. Berul, F. Cecchin, E. P. Walsh, J. K. Triedman, M. E. Alexander, *Heart Rhythm* **2004**, *1*, 150.
- [13] J. Rivnay, R. M. Owens, G. G. Malliaras, *Chem. Mater.* **2014**, *26*, 679.
- [14] A. Campana, T. Cramer, D. T. Simon, M. Berggren, F. Biscarini, *Adv. Mater.* **2014**, *26*, 3874.
- [15] M. Isik, T. Lonjaret, H. Sardon, R. Marcilla, T. Herve, G. G. Malliaras, E. Ismailova, D. Mecerreyes, *J. Mater. Chem. C* **2015**, *3*, 8942.
- [16] D. Pani, A. Dessi, J. F. Saenz-Cogollo, G. Barabino, B. Fraboni, A. Bonfiglio, *IEEE Trans. Biomed. Eng.* **2016**, *63*, 540.
- [17] K. He, Z. Liu, C. Wan, Y. Jiang, T. Wang, M. Wang, F. Zhang, Y. Liu, L. Pan, M. Xiao, H. Yang, X. Chen, *Adv. Mater.* **2020**, *32*, 2001130.
- [18] H. U. Chung, A. Y. Rwei, A. Hourlier-Fargette, S. Xu, K. Lee, E. C. Dunne, Z. Xie, C. Liu, A. Carlini, D. H. Kim, D. Ryu, E. Kulikova, J. Cao, I. C. Odland, K. B. Fields, B. Hopkins, A. Banks, C. Ogle, D. Grande, J. B. Park, J. Kim, M. Irie, H. Jang, J. Lee, Y. Park, J. Kim, H. H. Jo, H. Hahm, R. Avila, Y. Xu, et al, *Nat. Med.* **2020**, *26*, 418.
- [19] M. Oehler, M. Schilling, H. D. Esperer, *Biomed. Tech* **2009**, *54*, 329.
- [20] J. Liu, X. Zhang, Y. Liu, M. Rodrigo, P. D. Loftus, J. Aparicio-Valenzuela, J. Zheng, T. Pong, K. J. Cyr, M. Babakhanian, J. Hasi, J. Li, Y. Jiang, C. J. Kenney, P. J. Wang, A. M. Lee, Z. Bao, *Proc. Natl. Acad. Sci. USA* **2020**, *117*, 14769.
- [21] D.-H. Kim, N. Lu, R. Ma, Y.-S. Kim, R.-H. Kim, S. Wang, J. Wu, S. M. Won, H. Tao, A. Islam, K. J. Yu, T.-i. Kim, R. Chowdhury, M. Ying, L. Xu, M. Li, H.-J. Chung, H. Keum, M. McCormick, P. Liu, Y.-W. Zhang, F. G. Omenetto, Y. Huang, T. Coleman, J. A. Rogers, *Science* **2011**, *333*, 838.
- [22] J. Rivnay, S. Inal, A. Salleo, R. M. Owens, M. Berggren, G. G. Malliaras, *Nat. Rev. Mater.* **2018**, *3*, 17086.
- [23] P. Lin, F. Yan, *Adv. Mater.* **2012**, *24*, 34.
- [24] E. Bihar, T. Roberts, M. Saadaoui, T. Hervé, J. B. De Graaf, G. G. Malliaras, *Adv. Healthcare Mater.* **2017**, *6*, 1601167.
- [25] H. Liu, A. Yang, J. Song, N. X. Wang, P. Lam, Y. Li, H. K.-W. Law, F. Yan, *Sci. Adv.* **2021**, *7*, eabg8387.
- [26] S. Inal, G. G. Malliaras, J. Rivnay, *Nat. Commun.* **2017**, *8*, 1767.
- [27] D. Khodagholy, T. Doublet, P. Quilichini, M. Gurfinkel, P. Leleux, A. Ghestem, E. Ismailova, T. Hervé, S. Sanaur, C. Bernard, G. G. Malliaras, *Nat. Commun.* **2013**, *4*, 1575.
- [28] J. Rivnay, P. Leleux, M. Ferro, M. Sessolo, A. Williamson, D. A. Koutsouras, D. Khodagholy, M. Ramuz, X. Strakosas, R. M. Owens, C. Benar, J.-M. Badier, C. Bernard, G. G. Malliaras, *Sci. Adv.* **2015**, *1*, e1400251.
- [29] M. Ganji, E. Kaestner, J. Hermiz, N. Rogers, A. Tanaka, D. Cleary, S. H. Lee, J. Snider, M. Halgren, G. R. Cosgrove, B. S. Carter, D. Barba, I. Uguz, G. G. Malliaras, S. S. Cash, V. Gilja, E. Halgren, S. A. Dayeh, *Adv. Funct. Mater.* **2017**, *28*, 1700232.
- [30] V. Venkatraman, J. T. Friedlein, A. Giovannitti, I. P. Maria, I. McCulloch, R. R. McLeod, J. Rivnay, *Adv. Sci.* **2018**, *5*, 1800453.
- [31] G. D. Spyropoulos, J. N. Gelinas, D. Khodagholy, *Sci. Adv.* **2019**, *5*, eaau7378.
- [32] P. Leleux, J. Rivnay, T. Lonjaret, J.-M. Badier, C. Bénar, T. Hervé, P. Chauvel, G. G. Malliaras, *Adv. Healthcare Mater.* **2015**, *4*, 142.
- [33] M. Braendlein, T. Lonjaret, P. Leleux, J.-M. Badier, G. G. Malliaras, *Adv. Sci.* **2017**, *4*, 1600247.
- [34] C. Yao, Q. Li, J. Guo, F. Yan, I. M. Hsing, *Adv. Healthcare Mater.* **2015**, *4*, 528.
- [35] X. Gu, C. Yao, Y. Liu, I. M. Hsing, *Adv. Healthcare Mater.* **2016**, *5*, 2345.
- [36] H. Lee, S. Lee, W. Lee, T. Yokota, K. Fukuda, T. Someya, *Adv. Funct. Mater.* **2019**, *29*, 1906982.
- [37] E. Ajdaraga, M. Gusev, presented at *2017 25th Telecommunication Forum (TELFOR)*, Belgrade, Serbia Nov. **2017**.
- [38] L. Chen, Y. Fu, N. Wang, A. Yang, Y. Li, J. Wu, H. Ju, F. Yan, *ACS Appl. Mater. Interfaces* **2018**, *10*, 18470.
- [39] N. Wang, Y. Liu, Y. Fu, F. Yan, *ACS Appl. Mater. Interfaces* **2017**, *10*, 25834.
- [40] L. Q. Flagg, R. Giridharagopal, J. Guo, D. S. Ginger, *Chem. Mater.* **2018**, *30*, 5380.
- [41] X. Wu, A. Surendran, J. Ko, O. Filonik, E. M. Herzig, P. Müller-Buschbaum, W. L. Leong, *Adv. Mater.* **2019**, *27*, 1805544.

- [42] D. A. Bernardis, G. G. Malliaras, *Adv. Funct. Mater.* **2007**, *17*, 3538.
- [43] A. Giovannitti, D. T. Sbircea, S. Inal, C. B. Nielsen, E. Bandiello, D. A. Hanifi, M. Sessolo, G. G. Malliaras, I. McCulloch, J. Rivnay, *Proc. Natl. Acad. Sci. USA* **2016**, *113*, 12017.
- [44] O. Kwon, J. Jeong, H. B. Kim, I. H. Kwon, S. Y. Park, J. E. Kim, Y. Choi, *Healthc. Inform. Res.* **2018**, *24*, 198.
- [45] J. Rivnay, S. Inal, B. A. Collins, M. Sessolo, E. Stavrinidou, X. Strakosas, C. Tassone, D. M. Delongchamp, G. G. Malliaras, *Nat. Commun.* **2016**, *7*, 11287.
- [46] D. E. Becker, *Anesth. Prog.* **2006**, *53*, 53.
- [47] M. S. Spach, R. C. Barr, J. W. Havstad, E. C. Long, *Circulation* **1966**, *34*, 649.
- [48] X.-L. Yang, G.-Z. Liu, Y.-H. Tong, H. Yan, Z. Xu, Q. Chen, X. Liu, H.-H. Zhang, H.-B. Wang, S.-H. Tan, *J. Geriatr. Cardiol.* **2015**, *12*, 448.
- [49] J. K. Cooper, *N. Engl. J. Med.* **1986**, *315*, 461.
- [50] F. N. Wilson, A. G. Macleod, P. S. Barker, *Am. Heart. J.* **1931**, *7*, 207.